Importance of creeping waves in Schwinger variational-principle calculations of backscattering from cylinders with Neumann's boundary condition

B. J. Stoyanov and R. A. Farrell
The Johns Hopkins University Applied Physics Laboratory, Laurel, Maryland 20723-6099
(Received 15 May 1996)

The Schwinger variational principle for the scattering amplitude produces accurate results when the trial function is selected to contain the essential physics of the problem. Very simple trial functions that are capable of satisfying the boundary condition and of approximating the lit and unlit aspects of shadowing give excellent results for Dirichlet scatterers but not for Neumann scatterers. Physics suggests that creeping waves are the missing ingredient in the latter case. The current study verifies the validity of this suggestion for the test problem of plane-wave scattering from an infinite cylinder. The validation is based on a hybrid solution that consists of the variational backscattering amplitude supplemented by the creeping-wave contribution that is available from the exact solution. Good accuracy is obtained for the entire frequency range, thereby suggesting that incorporating the creeping-wave effects into the shadowed-boundary-Born trial functions is as much improvement as is needed and desirable in order to obtain good fully variational results for smooth scatterers with Neumann's boundary condition. [S1063-651X(96)00412-6]

PACS number(s): 42.25.Fx, 02.30.Wd, 03.50.De, 03.80.+r

I. INTRODUCTION

The well-known powerful feature of the Schwinger variational principle [1–6,7, pp. 1135 and 1545], which makes this or any other variational principle attractive in approximate calculations, is that the error in the approximation for the physical quantity of interest is of second order when the error in the trial function is of first order. Moreover, the variational principle is guaranteed to yield exact results if the trial function is exact. Conversely, when the error in the trial function is sufficiently large the error in the result becomes correspondingly augmented, and the variational principle fails dramatically.

In general, no bounds are available for determining the accuracy of the approximation [8, pp. 465, 577, and 653] in variationally formulated scattering problems because the Schwinger variational principle is neither a minimum nor a maximum, but merely a stationary principle with an unknown ''saddle'' orientation [9,10]. Consequently, greater complexity of trial functions does not guarantee greater final accuracy of variational results [6,9,10], and a judicious choice of trial functions is of great importance for scattering problems. The use of simple test problems to guide the development of generic trial functions and to verify their overall efficacy has proven beneficial.

Therefore, in our quest for finding trial functions that are simple and plausible rather than formal and rigorous [11,12], [13, Sec. I.2.14.2], [14, Sec. 2.2.2.6], we have relied [15–19] on generic insights into the physical aspects of wave-scattering problems, and tested these insights with simple canonical problems for which exact solutions are available [13,14]. In view of the lack of specific criteria for the successful choice of trial functions [12], it has been suggested [20] that one should make every effort to select trial functions that satisfy as many of the known features of the solution as possible. However, our previous work on wave scattering suggests that, with Dirichlet's boundary condition (TM polarization), it is sufficient for the trial functions to be capable of only *crudely* imitating the *essential* physical requirements of the problem at hand, at least for the problems examined [15–19]. More specifically, with the shadowed-boundary-Born trial functions that are capable of imitating (even rather crudely) both the correct boundary condition on the scatterer surface and the expected shadowing effects of the obstacle, very good all-frequency accuracy can be obtained for plane-wave scattering from acoustically soft spheres [16] and spheroids [17], as well as from perfectly conducting cylinders and hemicylindrically embossed planes [18,19].

Before investing the considerable effort needed to develop numerical and analytical techniques for optimal evaluation of the variational principle in practical problems, it is desirable to examine whether additional physics needs to be included in the design of trial functions for other boundary conditions. This paper concentrates on a simple test problem of plane-wave backscattering from an infinite cylinder with Neumann's boundary condition (TE polarization). Specifically, it is demonstrated, via a hybrid solution, that when a creeping-wave contribution (which is available from the exact solution to the test problem) is added to the variationally derived backscattering amplitude, good accuracy results for the entire frequency range. Thereby this paper demonstrates that, unlike the TM case where the creeping-wave effects are numerically insignificant, they represent an essential physical ingredient of the TE scattering that needs to be incorporated into the shadowed-boundary-Born trial functions.

II. THE OPTICS AND CREEPING-WAVE COMPONENTS OF THE EXACT BACKSCATTERING AMPLITUDE

Scattering of a plane wave from an infinitely long perfectly conducting cylinder of radius a is depicted in Fig. 1, where $\vec{k}_i$, $\vec{k}_s$ are, respectively, the incident and scattered

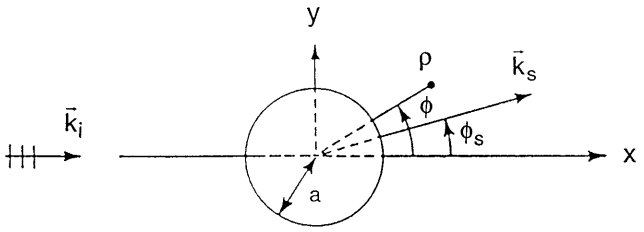

FIG. 1. Schematic representation of plane-wave scattering by an infinite cylinder. The incident electric field is along the y axis (TE polarization).

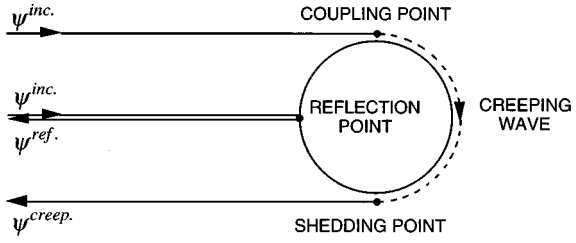

FIG. 2. Schematic illustration of the specularly reflected ray and a creeping wave, whose interference produces oscillations in the exact backscatter.

propagation vectors (with $k_s=k_i\equiv k=2\pi/\lambda$, and λ the incident wavelength). As denoted in Fig. 1, the scattering angle ϕ_s is measured from the incident direction (x axis), and the cylinder axis is along the z direction. The usual polar coordinates ρ, ϕ are used to specify an arbitrary point ($\vec{\rho}$) in a plane normal to the cylinder axis. Only normal plane-wave incidence is considered because, for the case of a perfect conductor, a general three-dimensional (3D) problem of oblique incidence can be reduced to two scalar (i.e., TM and TE) 2D scattering problems [13, p. 90]. Also, without loss of generality, the incident plane wave is assumed to be of unit (dimensionless) amplitude, and the harmonic time dependence $e^{-i\omega t}$ is suppressed everywhere.

For TE polarization, the total (incident plus scattered) scalar wave function ψ represents the (total) magnetic field that is parallel to the cylinder axis and has its normal derivative vanishing on the cylinder surface, i.e., satisfies Neumann's boundary condition. The far-zone scattered field is represented in terms of the dimensionless scattering amplitude $T(\phi_s)$ as [14, Sec. 4.1.1.2]

$$\psi_s(\rho,\phi_s)=\sqrt{2/\pi}\,\frac{e^{i(k\rho-\pi/4)}}{\sqrt{k\rho}}\,T(\phi_s), \tag{1}$$

where [14, Sec. 4.1.2.1]

$$T(\phi_s)=-\sum_{m=0}^{\infty}\varepsilon_m\,\frac{J_m'(ka)}{H_m^{(1)\prime}(ka)}\cos m\phi_s \tag{2a}$$

with

$$\varepsilon_m=\begin{cases}1, & m=0\\ 2, & m=1,2,\ldots\ .\end{cases} \tag{2b}$$

Here J_m and $H_m^{(1)}$ are, respectively, Bessel and Hankel functions of the first kind of order m [21, p. 358], and the primes indicate derivatives with respect to the argument. The differential cross section (cf. [14, Sec. 4.1.1.2])

$$\sigma=\begin{cases}|T|^2/(ka)^2 & \text{forward } (\phi_s=0), \quad (3a)\\ |T|^2(4/\pi ka) & \text{otherwise } (\phi_s\neq 0) \quad (3b)\end{cases}$$

is normalized so that $\sigma\to 1$ for forward scattering and back scattering when $ka\to\infty$.

Utilizing an elaborate asymptotic (large size parameter ka) analysis [22,23,14, Sec. 2.3.2], the exact backscattering ($\phi_s=\pi$) amplitude can be decomposed into its optical $T^{\rm op}$ and creeping-wave $T^{\rm cr}$ components [24, Sec. 17.41]

$$T=T^{\rm op}+T^{\rm cr}. \tag{4a}$$

A development useful numerically for $ka>2$ is explicitly given by [13, Sec. 2.2.2.3, 14, Sec. 4.1.2.4.2]:

$$T^{\rm op}=\tfrac{1}{2}\sqrt{\pi ka}\,\exp[i(\pi/4-2ka)]\times\left\{1-\frac{i11}{16ka}-\frac{353}{512(ka)^2}+O[(ka)^{-3}]\right\} \tag{4b}$$

and

$$T^{\rm cr}=1.531\,915\sqrt{\pi}(ka)^{1/3}\exp[-2.20(ka)^{1/3}-0.395\,763\,5(ka)^{-1/3}]\exp\{i[\pi/3+\pi ka+1.270\,169\,5(ka)^{1/3}-0.228\,494\,5(ka)^{-1/3}]\}. \tag{4c}$$

The first term in the optical component is the standard geometric optics contribution, which is shown in Fig. 2 as a specularly reflected ray. The physical interpretation of the origin of the far-field creeping-wave contribution (4c) is as follows [14, Sec. 2.3.2, 22,23,24, Secs. 17.32 and 17.41]. The incident rays at the two points of tangency to the cylinder (see Fig. 2 where only one such ray is shown) launch creeping waves that travel along the cylinder surface with the phase velocity slightly smaller than in free space. As they travel along the surface, they shed radiation along tangential directions and thus become exponentially damped.

One can readily appreciate the accuracy of the optics and creeping-waves representation (4) of the exact backscatter through inspection of Fig. 3. In this figure, backscattering cross sections for the optics contribution, the creeping-wave contribution, and the combined optics plus creeping-wave contribution, as generated by substituting Eqs. (4) into Eq. (3b), are plotted along with the exact solution. The representation (4) fails badly for $ka\lesssim 1$, but is quite accurate for $ka\gtrsim 2$, becoming progressively more accurate with increasing ka.

The main features of the backscatter oscillatory structure can be readily deduced [22,25, Sec. 4.3.1, 26, Sec. 6.2.1] from a simple physical representation of interference between the specularly reflected wave and a creeping wave that encircles the cylinder to the other point of tangency and is shed backwards (Fig. 2). To the extent that the creeping wave travels along the cylinder surface at (approximately)

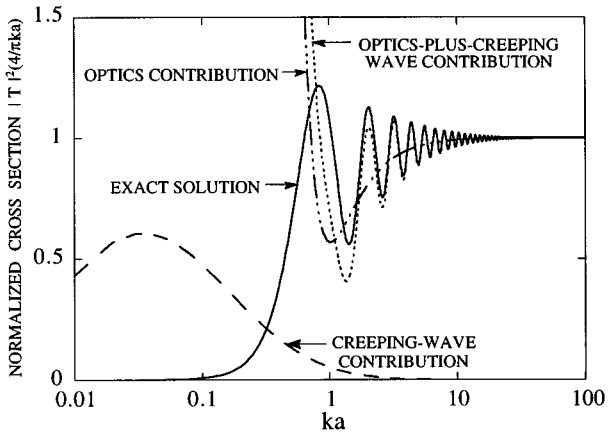

FIG. 3. The optics (dot-dashed curve), creeping-wave (dashed curve), and optics-plus-creeping-wave (dotted curve) approximations are compared with the exact backscatter (solid curve). The optics-plus-creeping-wave approximation of the exact solution is quite accurate for $ka \gtrsim 2$ but fails at small ka's. The logarithmic ka scale is used to emphasize the small and moderate ka behavior.

the free-space velocity, it traverses an additional (relative to the specularly reflected ray) path length equal to the cylinder diameter plus half the circumference, or a total additional path of $(2+\pi)a$. The interference pattern, therefore, should have peak-to-peak spacings in ka that occur when the path length difference is a wavelength, or for $\Delta ka = 2\pi/(2+\pi) \approx 1.22$, which is in close agreement with the actual average spacing in Fig. 3. Furthermore, because the creeping wave loses energy in proportion to the distance traveled along the cylinder, it becomes weaker (damped) as the cylinder radius becomes larger. Consequently, the interference pattern becomes weaker (damped) as the electrical size of the cylinder, i.e., its size parameter ka, increases. Therefore, the creeping-wave contribution becomes numerically insignificant for $ka \gtrsim 20$. Also, the higher-order creeping waves that made one or more additional complete circumnavigations in clockwise and counterclockwise directions around the cylinder are of little significance, and were not included in Eq. (4c).

We note in passing that in the corresponding expression for creeping waves with TM polarization [13, Sec. 2.2.1.3, 14, Sec. 4.1.2.4.2] the numerical coefficient (-2.20) in the exponent of the dominant damping factor in Eq. (4c) would be replaced by (≈ -5.05), and the overall constant factor (≈ 1.53) by (≈ 0.91), among other minor changes. Consequently, the creeping-wave contribution is numerically insignificant for TM polarization, and produces only a slight, barely perceptible wavering in the backscatter as a function of ka.

III. SCHWINGER VARIATIONAL PRINCIPLE FOR SCATTERING AMPLITUDE

The Schwinger variational principle for wave scattering from a cylinder with Neumann's boundary condition (TE polarization) can be readily derived following the standard procedure [2–6, 7, pp. 1135 and 1545]. The resulting variational expression for the (complex) scattering amplitude

$$T^V = N\tilde{N}/D \tag{5a}$$

can be written down in terms of line integrals along the cylinder circumference

$$N = \frac{ia}{4} \int_0^{2\pi} d\phi \; \psi(\rho,\phi) \frac{\partial}{\partial \rho} e^{-ik\rho \cos(\phi-\phi_s)} \Big|_{\rho=a}, \tag{5b}$$

$$\tilde{N} = \frac{ia}{4} \int_0^{2\pi} d\phi' \, \tilde{\psi}(\rho',\phi') \frac{\partial}{\partial \rho'} e^{ik\rho' \cos\phi'} \Big|_{\rho'=a}, \tag{5c}$$

$$D = \frac{a^2}{16} \int_0^{2\pi} d\phi \int_0^{2\pi} d\phi' \, \psi(\rho,\phi)\tilde{\psi}(\rho',\phi') \times \frac{\partial^2 H_0^{(1)}(k|\vec{\rho}-\vec{\rho}'|)}{\partial\rho\partial\rho'} \Big|_{\substack{\rho=a \\ \rho'=a}}. \tag{5d}$$

Here, as in Sec. II the scalar wave function ψ represents the total (incident plus scattered) magnetic field that is parallel to the cylinder axis z. Also, $\tilde{\psi}$ represents the adjoint field, i.e., the solution of the reciprocal problem in which the source and observer are interchanged [7, p. 1131]. It should be noted that the variational solution will satisfy reciprocity [11] if the adjoint trial field is chosen via the substitution $\phi - \phi_i \to \phi - \phi_s - \pi$, i.e.,

$$\tilde{\psi}^{\text{trial}}(\rho',\phi') = \psi^{\text{trial}}(\rho,\phi)\big|_{\phi=\phi'-\phi_s-\pi}, \tag{6}$$

where the incident angle is eliminated ($\phi_i = 0$) by measuring all angles relative to it (see Fig. 1). This choice for the adjoint trial field is used throughout this paper. The Hankel function of the first kind and zeroth order, $H_0^{(1)}$, in Eq. (5d) represents (up to a constant factor) a 2D free-space Green's function appropriate for this problem [13, Sec. I.2.7]. The variational cross section σ^V is found from Eq. (3) with T^V substituted for T.

If the correct field ψ (and, hence, $\tilde{\psi}$) on the scatterer surface is used in Eq. (5), each of the integrals N, $\tilde{N}$, and D, as well as their ratio Eq. (5a), will yield the correct scattering amplitude. However, in general, such correct surface fields are not known, which necessitates the use of approximations for ψ (and its adjoint) on the scatterer surface to obtain an approximate variational scattering amplitude T^V.

IV. VARIATIONAL SOLUTION WITH THE SHADOWED-BOUNDARY-BORN TRIAL FUNCTION

The approach we used to develop the boundary-Born trial functions with shadowing has been described in detail in [19], so here we just recapitulate its salient features. Briefly, it is based on gaining physical insight into scattering problems, in particular for limiting cases such as very small and very large size parameters ka, and then to incorporate the essential physics into the trial function. In this approach, starting with the classic Born approximation (i.e., just the incident-wave field) as a ''seed,'' a single universal trial function capable of correctly reproducing both the small and large ka limits, as well as to (crudely) imitate the essential

physical requirements of the problem, is designed for the entire frequency range.

In this section we only state the results for TE scattering, with the main focus being on the backscatter, which is of prime interest in monostatic radar measurements [14, p. 9]. The following shadowed-boundary-Born trial function

$$\psi(\rho,\phi)=[1-\beta(ka)\cos\phi][e^{ik\rho\cos\phi}-f(k\rho)\cos\phi e^{ika\cos\phi}] \tag{7}$$

is used only in the immediate neighborhood of the cylinder and is capable of satisfying Neumann's boundary condition, i.e.,

$$\psi'(ka)\equiv\partial\psi(k\rho)/\partial\rho|_{\rho=a}=0, \tag{8}$$

provided $f'(ka)=ik$. Thus, augmenting the incident plane wave (i.e., the classic Born approximation) with the $f(k\rho)$ term enables the trial function to satisfy the correct boundary condition that is known to play a key role at low and moderate frequencies [27]. The quantity that actually enters the invariant expression (5) for the scattering amplitude is $f(ka)$. The factor $[1-\beta(ka)\cos\phi]$ is a (crude) approximation to geometric shadowing in that, for positive β near unity, this factor is small for ϕ near zero and is $(1+\beta)$ for ϕ near π. The adjoint trial field follows from Eq. (6), which implies that $\tilde{\beta}=\beta$ and $\tilde{f}(ka)=f(ka)$.

Inserting the trial function (7) and its adjoint into Eq. (5), and using Graf's addition theorem [21, p. 363] at the cylinder surface in order to reduce the double integral in Eq. (5d) to a sum of products of two single integrals, we obtain

$$\begin{aligned}N=&-ka(i\pi/2)\left\{\sin\frac{\phi_s}{2}J_1(\alpha)-i\frac{\beta}{2}[\cos\phi_s J_0(\alpha)\right.\\&+J_2(\alpha)]-\frac{i}{2}f(ka)\left(\cos\phi_s J_0(\alpha)+J_2(\alpha)\right.\\&+i\beta\left[\left(\sin\frac{\phi_s}{2}-\frac{1}{2}\sin\frac{3\phi_s}{2}\right)J_1(\alpha)\right.\\&\left.\left.\left.-\frac{1}{2}\sin\frac{\phi_s}{2}J_3(\alpha)\right]\right)\right\}\end{aligned} \tag{9a}$$

and

$$\begin{aligned}D=&k^2a^2(\pi^2/4)\sum_{m=0}^{\infty}\varepsilon_m\cos(m\phi_s)J_m'H_m^{(1)\prime}\\&\times[J_m+i\beta J_m'+if(ka)(J_m'+i\beta J_m'')]^2,\end{aligned} \tag{9b}$$

where

$$\alpha\equiv 2ka\,\sin(\phi_s/2), \tag{9c}$$

and the arguments of Bessel and Hankel functions in Eq. (9b) are understood to be ka, with the primes indicating derivatives with respect to the argument. We also note that due to the choice Eq. (6), $\tilde{N}=N$. It is convenient to write Eqs. (9a) and (9b) as

$$N\equiv n_0[n_1+n_2f(ka)] \tag{10a}$$

and

$$D\equiv d_0[d_1+2d_2f(ka)+d_3f^2(ka)], \tag{10b}$$

where n_0 and d_0 are the overall (angular-independent) factors in Eqs. (9a) and (9b), with explicit expressions for the other symbolic quantities being obvious from the termwise correspondence between Eqs. (10a) and (10b) and (9a) and (9b).

The as-yet arbitrary function $f(ka)$ is treated as a variational parameter being determined through the stationary condition

$$\partial T^V/\partial f(ka)=0. \tag{11}$$

Then it follows from Eq. (10) that the stationary $f(ka)$ can be expressed as

$$f(ka)=-\frac{n_1d_2-n_2d_1}{n_1d_3-n_2d_2}, \tag{12}$$

and the stationary scattering amplitude is

$$T^V=\frac{N^2}{D}=-\frac{n_1^2d_3-2n_1n_2d_2+n_2^2d_1}{d_1d_3-d_2^2}, \tag{13}$$

where the symbols $f(ka)$ and T^V are now used to denote the stationary values [28]. All of the quantities in Eqs. (12) and (13) are known, and reduce to simpler expressions for backscattering, $\phi_s=\pi$.

The first (shadowing) factor in Eq. (7), with $\beta(ka)$ assumed independent of ϕ, was introduced in order to imitate the shadowing effects that become important at high frequencies [7, pp. 1381 and 1551]. On the other hand, according to the physics of wave scattering, shadowing is not present for small size parameters because diffraction causes the entire scatterer to be illuminated. Therefore, we specify $\beta(ka)$ by introducing a simple ramp function as follows:

$$\beta(ka)=\begin{cases}0, & ka\leqslant 0.4\\(ka-0.4)/(1.0-0.4), & 0.4<ka<1.0\\1, & ka\geqslant 1.0.\end{cases} \tag{14}$$

Hence, for $ka\geqslant 1$, $\beta=1$ and the shadowing factor in Eq. (7) equals two at the central point on the illuminated side ($\phi=\pi$) of the cylinder, then gradually diminishes to zero at the opposite point ($\phi=0$) on the shadowed side, thus imitating correctly the expected shadowing effects at these points [29].

For $ka\leqslant 0.4$, $\beta=0$ and the trial function (7) goes over to the boundary-Born function without shadowing, which provides [by virtue of the stationary $f(ka)$ employed in Eq. (9)] variational results that are very accurate. In fact, the nonshadowed trial field, $\beta=0$, yields very accurate results for $ka\lesssim 0.7$. For moderate and large size parameters the nonshadowed trial function yields a backscatter that reasonably approximates the first few oscillations, but is heavily contaminated by spurious wiggles and/or narrow-band spikes beginning with ka somewhat larger than one, as illustrated in Fig. 4(c). Even so, this result is a marked improvement on the corresponding Born [whose scattering amplitude is represented by N with $\beta\equiv 0$ and $f(ka)\equiv 0$] and Born-variational [with $\beta\equiv 0$ and $f(ka)\equiv 0$ in Eq. (9)] approximations shown in Figs. 4(a) and 4(b), respectively.

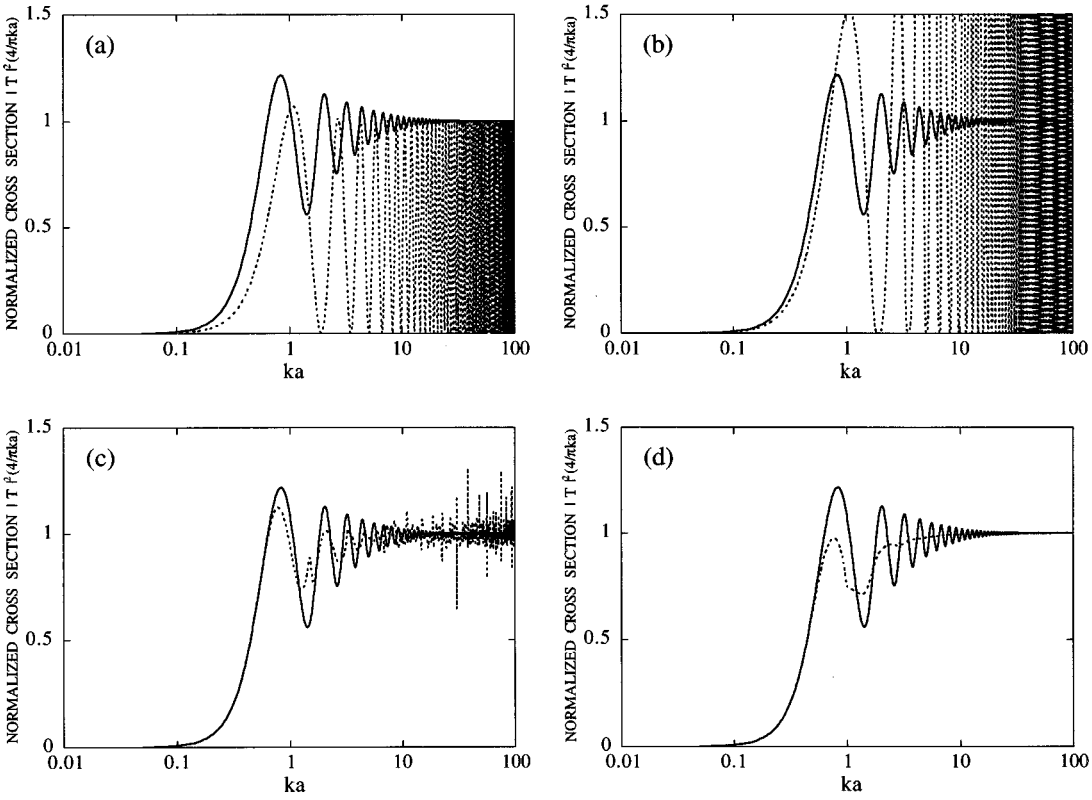

FIG. 4. The Born and Born-variational approximations (dotted curves) are compared with the exact backscatter (solid curve) in, respectively, (a) and (b). The variational results (dotted curves) calculated by using the boundary-Born trial function without and with shadowing are shown against the exact solution (solid curve) in, respectively, (c) and (d). Note that the variational result in (d) is very accurate for $ka \lesssim 0.6$ and $ka \gtrsim 20$, but lacks the interference pattern of the exact solution in the resonance region.

Furthermore, when the simple shadowing with $\beta(ka)$ defined in Eq. (14) is incorporated into the boundary-Born trial function [with the stationary $f(ka)$ determined by Eq. (11)] as in Eq. (7), the spurious features are effectively eliminated and the resulting backscatter is quite accurate for both small ($ka \lesssim 0.6$) and large ($ka \gtrsim 20$) size parameters, see Fig. 4(d). However, in between, i.e., in the resonance region ($0.4 \lesssim ka \lesssim 20$) [14, p. 147], where the exact solution attains a peak near $ka = 0.8$ and then oscillates about the geometric optics value of $\sigma = 1$ [see Eqs. (4b) and (3b)] with damped, regularly spaced excursions, the shadowed-boundary-Born trial field yields an approximate backscatter cross section that resembles an overall average of the exact result.

V. HYBRID (VARIATIONAL PLUS CREEPING WAVES) SOLUTION

In order to gain further insight into the behavior of the shadowed-boundary-Born backscatter, we compare both the cross sections and the (scattering amplitude) phases of the variational and optics approximations in Fig. 5. The variational result is very accurate for $ka \lesssim 0.6$ [Fig. 4(d)], but the optics approximation fails in this region (Fig. 3). However, an inspection of Fig. 5 reveals that the two approximations are in general agreement for $ka \gtrsim 2$, and they practically coincide for $ka \gtrsim 10$, both approaching the geometric optics limit for large ka. Coupling these observations with the fact that the optics-plus-creeping-wave approximation (Fig. 3) is reasonably accurate for $ka \gtrsim 2$, suggests that augmenting the variational backscatter with the creeping-wave contribution Eq. (4c), might lead to better accuracy.

It is gratifying to see this expectation amply fulfilled, as Fig. 6 attests, where the hybrid solution obtained by substituting [cf. Eq. (4a)]

$$T^{\mathrm{hyb}} = T^{V} + T^{\mathrm{cr}} \tag{15}$$

into Eq. (3b) is compared with the exact backscatter cross section and phase. Not only a remarkable improvement is achieved for $ka \gtrsim 2$, i.e., for the domain where the representation (4) holds true, but also the agreement is quite good for $0.6 \lesssim ka \lesssim 2.0$, where the creeping-wave theory is not supposed to be efficient (see Fig. 3). This somewhat unexpected improvement is, in part, a result of our use of the same ramp function as in Eq. (14) to premultiply T^{cr} (which is quite reasonable), but is mostly due to the fact that the shadowed-boundary-Born backscatter T^{V} is more accurate than the optics contribution T^{op} for $0.7 \lesssim ka \lesssim 2$ [cf. Figs. 3 and 4(d)]. And since T^{V} itself is very accurate for $ka \lesssim 0.6$ and $ka \gtrsim 20$, good all-frequency accuracy is achieved with this hybrid solution for TE backscattering.

On the other hand, for TM backscattering, we have found that the hybrid solution does not lead to further improvements of the already very accurate variational results [19].

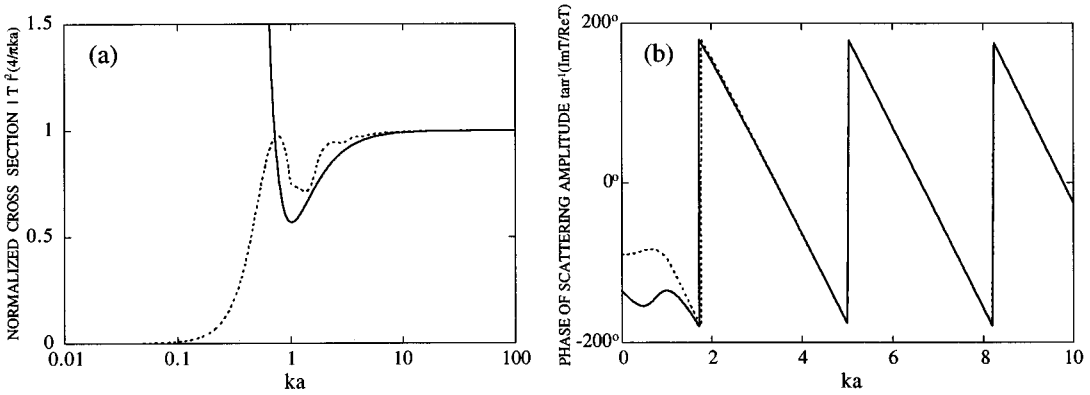

FIG. 5. Comparison of the (shadowed-boundary-Born) variational solution (dotted curve) and the optics approximation (solid curve). The cross sections are plotted in (a) and the (scattering amplitude) phases in (b). Note that while the variational and optics approximations are in general agreement with each other for $ka \gtrsim 2$, the variational result is also very accurate for $ka \gtrsim 0.6$ where the optics approximation fails, cf. Figs. 3 and 4(d).

This is because the nominal changes effected by the corresponding creeping-wave contribution [14, Sec. 4.1.2.4.2] are comparable to the existing small inaccuracies in the variational results. Therefore, unlike the TE case, for TM scattering further improvement in the shadowed-boundary-Born trial functions by (approximately) including the creeping-wave effects is unwarranted from a practical computational standpoint.

VI. SUMMARY AND CONCLUSIONS

In this paper, we have demonstrated for a simple test problem of plane-wave scattering from an infinite cylinder with Neumann's boundary condition that incorporating, via a hybrid solution, the creeping-wave contribution (available from the exact solution) into the variationally derived backscattering amplitude yields good accuracy for all size parameters. Intuitively appealing explanations have also been provided concerning the effectiveness of this hybrid (variational plus creeping waves) solution in the entire resonance region and beyond.

Although practical applicability of the hybrid approach is limited to those few scattering problems for which accurate and numerically efficient expressions for creeping-wave contributions are available, the present result nevertheless demonstrates that, for TE scattering, creeping waves constitute an essential physical ingredient missing in the shadowed-boundary-Born trial fields. Therefore, fully variational solutions need to be developed, whose trial functions would be capable of directly accommodating the creeping-wave effects through simple, approximate means similar to those used to imitate the correct boundary condition and the expected shadowing effects. It has also been observed that for TM scattering the shadowed-boundary-Born trial functions lead to very accurate variational results because creeping-wave effects are numerically insignificant in this case and need not be included into the trial functions.

It is our opinion that the shadowed-boundary-Born trial functions, with the creeping-wave effects properly (even if crudely) incorporated, should be sufficient to yield good broad-band accuracy for simple smooth scatterers with Neumann's boundary condition. However, additional work is needed in order to develop simple and efficient trial func-

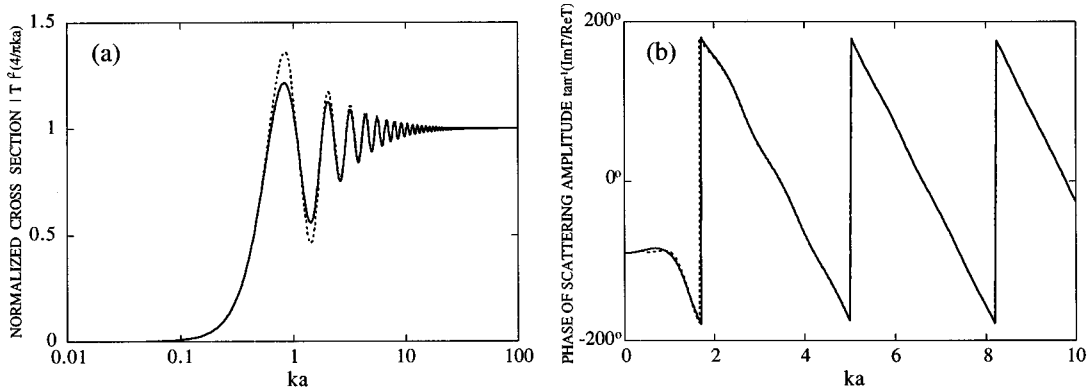

FIG. 6. Comparison of the hybrid (dotted curve) and the exact (solid curve) solutions. The cross sections are plotted in (a) and the (scattering amplitude) phases in (b). Note that, when the creeping-wave contribution (from the exact solution) is added to the scattering amplitude obtained from the (shadowed-boundary-Born) variational solution, the resulting hybrid solution yields good backscattering accuracy for all size parameters.

tions for problems of real interest, namely, general 3D problems with geometries not permitting exact analytical solutions. Moreover, the question of expediency of using the variational approach vs grinding out a numerical ''exact'' scattering amplitude arises.

ACKNOWLEDGMENTS

We thank S. Favin for his help with numerical computations. This work was supported by the U.S. Navy and the National Eye Institute.

[1] J. Schwinger, Phys. Rev. **72**, 742 (1947).
[2] H. Levine and J. Schwinger, Phys. Rev. **74**, 958 (1948).
[3] H. Levine and J. Schwinger, Phys. Rev. **75**, 1608 (1949).
[4] H. Levine and J. Schwinger, Pure Appl. Math. **3**, 355 (1950).
[5] H. Levine, *Variational Methods for Solving Electromagnetic Boundary Value Problems* (Sylvania Products Co., Mountain View, CA, 1954).
[6] E. Gerjuoy, A. R. P. Rau, and L. Spruch, Rev. Mod. Phys. **55**, 725 (1983).
[7] P. M. Morse and H. Feshbach, *Methods of Theoretical Physics* (McGraw-Hill, New York, 1953).
[8] D. S. Jones, *Methods in Electromagnetic Wave Propagation* (Clarendon, Oxford, 1979).
[9] C. D. Dolph, IRE Trans. Antennas Propag. **AP-4**, 302 (1956).
[10] C. D. Dolph, J. Soc. Ind. Appl. Math. **5**, 89 (1957).
[11] D. S. Jones, IRE Trans. Antennas Propag. **AP-4**, 297 (1956).
[12] D. S. Jones, Proc. IEE **121**, 573 (1974).
[13] *Electromagnetic and Acoustic Scattering by Simple Shapes*, edited by J. J. Bowman, T. B. A. Senior, and P. L. E. Uslenghi (Hemisphere, New York, 1987) (revised printing).
[14] *Radar Cross Section Handbook*, edited by G. T. Ruck (Plenum, New York, 1970).
[15] M. R. Feinstein and R. A. Farrell, J. Opt. Soc. Am. **72**, 223 (1982).
[16] D. E. Freund and R. A. Farrell, J. Acoust. Soc. Am. **87**, 1847 (1990).
[17] D. E. Freund and R. A. Farrell, J. Acoust. Soc. Am. **89 (2)**, 1994 (1991).
[18] R. A. Farrell *et al.*, JHU/APL Technical Report No. TG 1388, 1994 (unpublished).
[19] B. J. Stoyanov and R. A. Farrell, Phys. Rev. E **53**, 1907 (1996).
[20] A. D. Berk, IRE Trans. Antennas Propag. **AP-4**, 104 (1956).
[21] *Handbook of Mathematical Functions*, edited by M. Abramowitz and I. A. Stegun (Dover, New York, 1972).
[22] W. Franz and K. Depperman, Ann. Phys. **10**, 361 (1952).
[23] W. Franz and R. Galle, Z. Naturforsch. **10a**, 374 (1955).
[24] H. C. van de Hulst, *Light Scattering by Small Particles* (Dover, New York, 1981).
[25] M. Kerker, *The Scattering of Light and Other Electromagnetic Radiation* (Academic, New York, 1969).
[26] E. F. Knott, J. F. Shaeffer, and M. T. Tuley, *Radar Cross Section* (Artech House, Norwood, MA, 1985).
[27] D. T. Thomas, IEEE Trans. Microwave Theory Tech. **MTT-17**, 447 (1969).
[28] Symbolic expressions (12) and (13) hold also in the TM case and were actually used in [19] without being explicitly given there.
[29] We note in passing that, for TM scattering [19], the shadow-regulating parameter β was fixed by requiring that the correct large ka limit be obtained for the variational scattering amplitude in the forward direction. For TE scattering, our asymptotic analysis (using the results of [30]) shows that there is no physically reasonable β $(0<\beta\leqslant 1)$ that would provide the correct large ka limit for the forward scattering amplitude.
[30] B. J. Stoyanov, R. A. Farrell, and J. F. Bird, J. Comp. Appl. Math. **50**, 533 (1994).